Broadband terahertz wave generation from a $MgO:LiNbO_3$ ridge waveguide pumped by a 1.5 μm femtosecond fiber laser

Shuzhen Fan,[1,*] Hajime Takeuchi,[1] Toshihiko Ouchi,[2] Kei Takeya,[1] and Kodo Kawase[1,3]

[1]*Nagoya University, Furo-cho, Chikusa-ku, Nagoya 464-8601, Japan*

[2]*Canon Inc., Shimomaruko 3-chome, Ohta-ku, Tokyo 146-8501, Japan*

[3]*RIKEN, Aoba, Aramaki, Aoba-ku, Sendai, Miyagi 980-0845, Japan*

**Corresponding author: fanshuzhen@gmail.com*

Received March 4, 2013; revised April 11, 2013; accepted April 16, 2013;
posted April 16, 2013 (Doc. ID 186214); published May 9, 2013

Cherenkov phase-matched terahertz (THz) wave generation from a $MgO:LiNbO_3$ ridge waveguide was studied using optical rectification. Pumping was achieved using 20 and 60 fs laser pulses from a fiber laser centered at 1.56 μm. Time-domain spectroscopy (TDS) results showed a single-cycle pulse with 20 fs pulse pumping and a near-single-cycle pulse with 60 fs pulse pumping. The spectrum covered the range of 0.1–7 THz, with a signal-to-noise ratio of over 50 dB. The output power measured by a Si bolometer and a deuterated triglycine sulfate pyroelectric detector is shown and compared to that of a commercial photoconductive antenna. This system is believed to be a promising THz source for low-cost, compact, robust, and highly integrated TDS, THz imaging, and tomography systems.

OCIS codes: (140.3070) Infrared and far-infrared lasers; (190.7110) Ultrafast nonlinear optics; (300.6500) Spectroscopy, time-resolved.

http://dx.doi.org/10.1364/OL.38.001654

Terahertz time-domain spectroscopy (THz-TDS) has been widely used in many fields to investigate the physical, chemical, and dynamical properties of materials [1,2]. THz imaging [3] and THz tomography [4] have been widely employed in fields, such as homeland security, product quality control, and biological and medical imaging. The demand from these applications has stimulated rapid development of THz sources with high power, broadband spectra, and single-cycle temporal pulses.

One approach to broadband THz spectra is to use large-aperture photoconductive antennae (PCA) [5–7]. Another is the optical rectification (OR) of femtosecond laser pulses. Efforts have been made in many nonlinear materials, such as $LiNbO_3$ (LN) [8], GaP [9], DAST [10], OH1 [11], $ZnGeP_2$ [12], GaSe [13,14], ZnSe [15], and ZnTe [16]. However, these technologies all have at least one of the following drawbacks: high cost for pumping lasers, such as femtosecond Ti:sapphire lasers or self-made laser systems; commercially unavailable nonlinear crystals or materials; multicycle THz pulses; or the presence of gaps or narrowness in the spectrum.

LN is an excellent material that has been used in THz wave generation since the 1970s [17]. It has a high effective nonlinear coefficient and large bandgaps, making it possible to get high THz output [18]. However, its strong absorption in the THz band limits the output power. Many technologies have been developed to increase the efficiency and output power, such as the tilted-pulse-front technique [8], particular structures such as the Si–LN–air–metal sandwich structure [19,20], periodically poled LN (PPLN) [21], and LN slab waveguides [22].

In this Letter, we report the OR generation of high-power, broadband THz waves from MgO:LN ridge waveguides by Cherekov phase matching, pumped by a 1.56 μm femtosecond fiber laser. THz generation from LN ridge waveguides greatly decreases the absorption and the phase mismatching of THz waves [23]. This allows a longer working distance with higher pumping power density and results in high power and efficiency with a broadband spectrum. We report the THz power measured by a Si bolometer and a deuterated triglycine sulfate (DTGS) pyroelectric detector and compare the results with a commercial PCA. The TDS results showed a single-cycle pulse under 20 fs pulse pumping and a near-single-cycle pulse under 60 fs pumping in the temporal waveforms. The spectrum spanned from about 0.1 to 7 THz, with a signal-to-noise ratio (SNR) of over 50 dB. This system is a promising THz source for low-cost, compact, robust, and highly integrated TDS, THz imaging, and tomography systems.

The experimental setup is shown in Fig. 1. Dry air or nitrogen was not used during the entire experiment. The pumping laser source is a femtosecond fiber laser centered at 1.56 μm, which was reported by our group [24]. But the large mode-area fiber has been replaced by a new

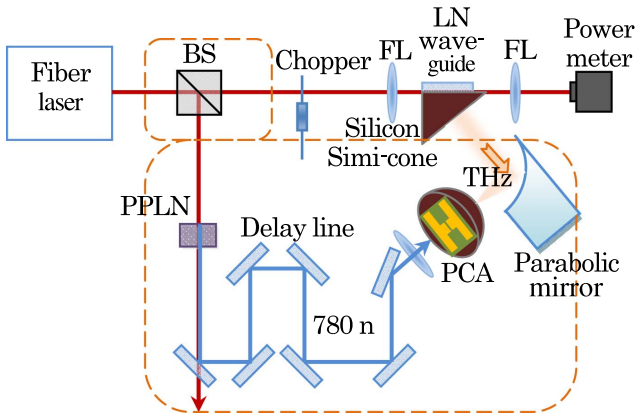

Fig. 1. Diagram of the experimental setup. BS, beam splitter; FL, aspherical focal lens. The objects inside the orange dashed boxes are only used for TDS measurements.

longer one and realignment was made for the current study. We used the 20 fs nonchirped laser after the second stage, as defined in [24], and the 60 fs prechirped laser, which had a higher power after the first stage. Although we used a self-made fiber laser, the experimental results showed that a commercial fiber laser is also appropriate for pumping. A coated aspherical lens (focal length $f = 4.5$ mm, working distance WD $= 2.4$ mm) was used to couple the laser to a 5 at. % MgO-doped LN ridge waveguide (dimensions 3.8 μm × 5 μm × 10 mm, NGK Insulator, Ltd.). The beam waist of the focused pumping beam is measured to be about 8 μm. Another lens was used to couple the laser from the waveguide to a power meter (Melles Griot) in order to use real laser power as the pumping power. A specially designed semi-cone silicon lens (with an apex angle of 40°) was used to couple and collimate the THz wave from the waveguide. The photographs of the waveguide and the silicon lens are shown in Fig. 2. A 3.5 μm thick polyethylene terephthalate film was inserted between the waveguide and the silicon lens to prevent leakage of the IR light from the waveguide.

A Si bolometer (Infrared Laboratories) and a DTGS detector were used to measure the THz output, respectively. A lock-in amplifier was used to decrease the noise and to enable measurements of the THz output from the PCA. The chopping frequency was 40 Hz for the Si bolometer and 23 Hz for the DTGS detector.

The THz output was measured using the Si bolometer with a gain of 200. The maximum output from the bolometer was limited by the lock-in amplifier (slightly above 1 V), but not the pumping power. The THz power from a commercial low-temperature-grown GaAs-based PCA (G10620-11, Hamamatsu) was also measured using the same Si bolometer with a gain of 1000. We used 10 V as the bias and tried to increase the pumping power to 15 mW using a 780 nm femtosecond fiber laser (Femtolite Ultra CS-20, IMRA), which was the maximum pumping limit for this PCA.

The responsivity of the bolometer is calibrated by using a blackbody (SR-2, CI-systems). Since the THz output was measured by the bolometer and the DTGS at the same time, the THz power from the DTGS is given based on the same calibration result. The THz output power results measured by the Si bolometer and the DTGS are all given in Fig. 3. The output data from the PCA were

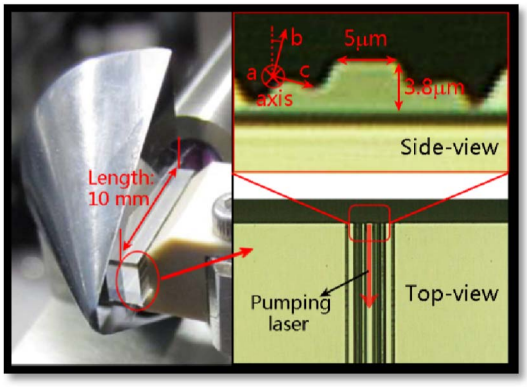

Fig. 2. Photograph of the LN ridge waveguide and the semi-cone silicon lens.

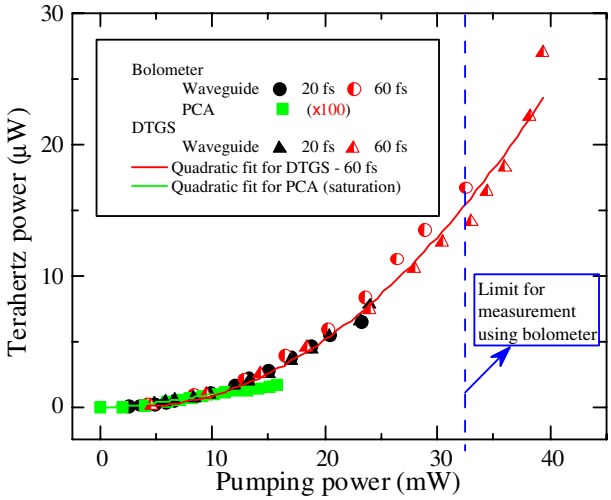

Fig. 3. THz output measured by a Si bolometer and a DTGS pyro-detector. The data for the PCA were multiplied by 100 for clarity. The blue dashed line indicates the maximum pumping for measurement with the bolometer, which was limited due to the saturation of the lock-in amplifier.

multiplied by 100 for viewing on the same graph. The symbols show the experimental results. The red solid curve shows the quadratic fitting for the results measured by DTGS detector with 60 fs pumping, based on the theory of OR [8], and the green curve shows the quadratic fitting for the PCA considering the saturation effect [6]. The maximum output from the waveguide was about 27 μW and was three orders of magnitude higher than that from PCA. The highest conversion efficiency we accomplished in this experiment is about 6.8×10^{-4}.

No saturation was observed, even at the maximum pumping power. This means that a higher output could be achieved with a more powerful laser. The output power under 20 and 60 fs pumping was almost the same for the results measured by the DTGS in Fig. 3 but differed slightly for the results measured by the bolometer. We believe it was due to the sensitivity variance each time liquid helium was added. Hence, the efficiency was insensitive to both pumping pulse widths that we used.

The pumping laser was separated into two beams by a 50/50 beam separator when performing TDS measurements, as shown in Fig. 1. So the TDS results are measured with half of the maximum power pumping for both pulse widths. A PPLN was used to get the second harmonic frequency laser at 780 nm, which was the pumping laser for the PCA (G10620-11, Hamamatsu). The THz wave from the waveguide was collected and focused into the PCA by a parabolic gold mirror.

The temporal pulses and the fast Fourier transform spectra are shown in Figs. 4(a) and 4(b), respectively. In Fig. 4(a), a single-cycle pulse was observed for the 20 fs pulse pumping, and a near-single-cycle pulse was observed for the 60 fs pulse pumping. The positive half-cycle of the THz amplitude has a width of about 127 fs at $1/\sqrt{2}$ of the peak for both pulse-width pumping values. Figure 4(b) shows a wide spectral span from about 0.1 to 7 THz, with an SNR of over 50 dB without gaps. The 60 fs data showed more energy at a higher frequency than the 20 fs data. We believe this is because

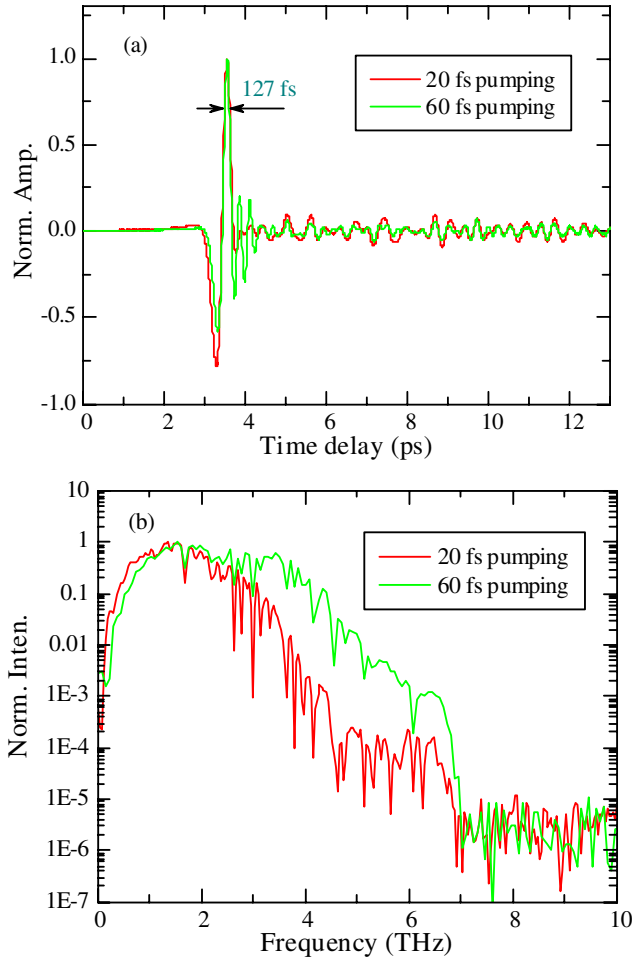

Fig. 4. (a) Temporal pulses and (b) spectrum from TDS measurement.

of the prechirping property of the 60 fs laser, together with the positive dispersion of the LN waveguide for the 1.56 μm laser.

To summarize, we showed broadband THz wave generation from a MgO:LN ridge waveguide pumped by a 1.5 μm femtosecond fiber laser. The output power of a Si bolometer was about three orders of magnitude higher than that of a commercial PCA. The spectrum ranged from about 0.1 to 7 THz with an SNR of over 50 dB without gaps. We believe that this is a promising THz source for low-cost, compact, robust, and highly integrated TDS, THz imaging, or tomography systems.

This work was supported by the Japan Science and Technology Agency (JST). We thank Professor M. Nagai in Osaka University for discussions. We thank Professor N. Nishizawa in Nagoya University for work on the fiber laser.

References

1. M. Theuer, S. S. Harsha, D. Molter, G. Torosyan, and R. Beigang, Chem. Phys. Chem. **12**, 2695 (2011).
2. M. Tonouchi, Nat. Photonics **1**, 97 (2007).
3. D. M. Mittleman, R. H. Jacobsen, and M. C. Nuss, IEEE J. Sel. Top. Quantum Electron. **2**, 679 (1996).
4. D. M. Mittleman, S. Hunsche, L. Boivin, and M. C. Nuss, Opt. Lett. **22**, 904 (1997).
5. Y. Gao, C.-E. Yang, Y. Chang, J. Yao, S. Yin, C. Luo, P. Ruffin, C. Brantley, and E. Edwards, Appl. Phys. B **109**, 133 (2012).
6. S. Winnerl, J. Infrared Millim. Terahertz Waves **33**, 431 (2012).
7. Y. C. Shen, P. C. Upadhya, H. E. Beere, E. H. Linfield, A. G. Davies, I. S. Gregory, C. Baker, W. R. Tribe, and M. J. Evans, Appl. Phys. Lett. **85**, 164 (2004).
8. M. C. Hoffmann and J. A. Fülöp, J. Phys. D **44**, 083001 (2011).
9. I. D. Vugmeyster, J. F. Whitaker, and R. Merlin, Appl. Phys. Lett. **101**, 181101 (2012).
10. K. Kawase, S. Ichino, K. Suizu, and T. Shibuya, J. Infrared Millim. Terahertz Waves **32**, 1168 (2011).
11. C. Ruchert, C. Vicario, and C. P. Hauri, Opt. Lett. **37**, 899 (2012).
12. J. D. Rowley, J. K. Pierce, A. T. Brant, L. E. Halliburton, N. C. Giles, P. G. Schunemann, and A. D. Bristow, Opt. Lett. **37**, 788 (2012).
13. W.-C. Chu, S. A. Ku, H. J. Wang, C. W. Luo, Y. M. Andreev, G. Lanskii, and T. Kobayashi, Opt. Lett. **37**, 945 (2012).
14. R. Huber, A. Brodschelm, F. Tauser, and A. Leitenstorfer, Appl. Phys. Lett. **76**, 3191 (2000).
15. Z. Lü, D. Zhang, Z. Zhou, L. Sun, Z. Zhao, and J. Yuan, Appl. Opt. **51**, 676 (2012).
16. S. Xu, J. Liu, G. Zheng, and J. Li, Opt. Express **18**, 22625 (2010).
17. K. H. Yang, P. L. Richards, and Y. R. Shen, Appl. Phys. Lett. **19**, 320 (1971).
18. K. Kawase, M. Sato, K. Nakamura, T. Taniuchi, and H. Ito, Appl. Phys. Lett. **71**, 753 (1997).
19. M. I. Bakunov, E. A. Mashkovich, M. V. Tsarev, and S. D. Gorelov, Appl. Phys. Lett. **101**, 151102 (2012).
20. S. B. Bodrov, I. E. Ilyakov, B. V. Shishkin, and A. N. Stepanov, Appl. Phys. Lett. **100**, 201114 (2012).
21. C. Zhang, Y. Avetisyan, A. Glosser, I. Kawayama, H. Murakami, and M. Tonouchi, Opt. Express **20**, 8784 (2012).
22. K. Suizu, K. Koketsu, T. Shibuya, T. Tsutsui, T. Akiba, and K. Kawase, Opt. Express **17**, 6676 (2009).
23. K. Takeya, K. Suizu, H. Sai, T. Ouchi, and K. Kawase, IEEE J. Sel. Top. Quantum Electron. **19**, 8500212 (2013).
24. J. Takayanagi, S. Kanamori, K. Suizu, M. Yamashita, T. Ouchi, S. Kasai, H. Ohtake, H. Uchida, N. Nishizawa, and K. Kawase, Opt. Express **16**, 12859 (2008).